

Density and spin response functions in ultracold fermionic atom gases

Bogdan Mihaila,¹ Sergio Gaudio,^{2,1} Krastan B. Blagoev,¹
 Alexander V. Balatsky,¹ Peter B. Littlewood,³ and Darryl L. Smith¹

¹*Theoretical Division, Los Alamos National Laboratory, Los Alamos, NM 87545*

²*Department of Physics, Boston College, Chestnut Hill, MA 02167*

³*Cavendish Laboratory, Madingley Road, Cambridge CB3 0HE, United Kingdom*

We propose a new method of detecting the onset of superfluidity in a two-component ultracold fermionic gas of atoms governed by an attractive short-range interaction. By studying the two-body correlation functions we find that a measurement of the momentum distribution of the density and spin response functions allows one to access separately the normal and anomalous densities. The change in sign at low momentum transfer of the density response function signals the transition between a BEC and a BCS regimes, characterized by small and large pairs, respectively. This change in sign of the density response function represents an unambiguous signature of the BEC to BCS crossover. Also, we predict spin rotational symmetry-breaking in this system.

PACS numbers: 03.75.Hh, 03.75.Ss, 05.30.Fk

The BEC-to-BCS crossover has drawn renewed interest in recent years due to experimental progress in atom trap systems [1]. Several groups [2] achieved a Bose-Einstein condensate (BEC) in which the fermions form non-overlapping (Shafroth) pairs [3] in a two-component Fermi gas. Despite considerable effort, much work is still needed to understand the other limit in which the pairs are large, and the pairing occurs in momentum space, similarly to the Bardeen-Cooper-Schrieffer (BCS) state of superconductivity in normal metals. Questions still remain regarding whether or not the system is superfluid when passing through the crossover with temperatures of the order of twenty percent of the Fermi temperature. The appropriate characterization of the system is still open to debate. Recently, several groups have claimed [4, 5] to have reached the superfluid state on the negative scattering length side of the Feshbach resonance. Despite evidence of fermionic pairing, these claims are still subject to intense discussions as no definitive proof of superfluidity [5] is available yet.

Viverit *et al.* [6] have suggested recently that the shape of the atomic momentum distribution at low temperatures is very sensitive to the sign and size of the scattering length. Altman *et al.* have proposed to utilize density-density correlations in the image of an expanding gas cloud to probe complex many-body states of trapped ultracold atoms. Also, Bruun and Baym [7] showed that scattered light from a fermionic gas would exhibit a large maximum below the superfluid critical temperature and therefore it can be used to detect the superfluid transition. However it is not clear how this behavior changes close to the crossover, where the actual experiments are performed.

In this paper we propose a new diagnostic method for fermionic atomic gas condensates. By studying the zero-temperature evolution of the density and spin response functions, as a function of the scattering length of the interaction, we show that the density response function

changes sign across the BEC to BCS crossover and that this change can be used to experimentally distinguish the BEC from the BCS state of the system.

Our model system consists of fermionic atoms in two hyperfine states interacting via a finite-range attractive interaction. Based on a variational approach, we also derive a sum-rule satisfied by the spin-spin correlation function at $q = 0$. We find that the density and spin response functions are given by the sum and the difference of independent contributions arising from the normal and anomalous density, respectively. By measuring the momentum distribution of the two response functions it is possible to infer separately the normal and anomalous densities. Finally, we predict symmetry breaking of the spin-rotation invariance. This prediction is characteristic to our model and, therefore, provides an experimental check for its applicability to real systems.

We begin by considering the two-body Hamiltonian

$$\mathbf{H} = \epsilon_{ki} \mathbf{a}_{ki}^\dagger \mathbf{a}_{ki} + \frac{1}{2} V_{q;im,nj} \mathbf{a}_{km}^\dagger \mathbf{a}_{pi}^\dagger \mathbf{a}_{p-qj} \mathbf{a}_{k+qn}, \quad (1)$$

where $\{\mathbf{a}_{ki}^\dagger, \mathbf{a}_{ki}\}$ are the *particle* creation and annihilation operators corresponding to single-particle states of linear momentum \mathbf{k} and fermion type i . The atomic levels, which we associate with the fermion types, are eigenstates of the Hamiltonian of an ion (with integer nuclear spin I) interacting with an electron (spin $s = \frac{1}{2}$)

$$\hat{H}_{\text{atom}} = k.e. + A \vec{s} \cdot \vec{I} + \vec{B} \cdot (2\mu_e \vec{s} - \mu_n \vec{I}), \quad (2)$$

where A denotes the strength of the hyperfine interaction and \vec{B} is the magnetic field, while μ_e and μ_n denote the electron and nuclear magnetic moments, respectively. We introduce the total angular momentum, $\vec{F} = \vec{I} + \vec{s}$. The total angular momentum projection, M_F , is the only good quantum number at finite B . The atomic spectra considered in our model are depicted in Fig. 1.

In the Hartree-Fock-Bogoliubov (HFB) formalism, one first introduces the *quasi-particle* creation and annihilation

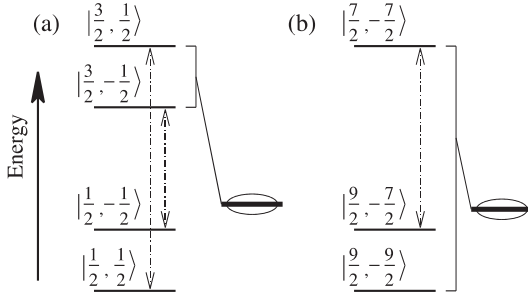


FIG. 1: Atomic states involved in the Feshbach resonance at small magnetic field, B , for (a) ${}^6\text{Li}$ and (b) ${}^{40}\text{K}$. The hyperfine couplings between states allowed by the selection rules are represented by dotted lines. In ${}^6\text{Li}$, the bound state is formed from the $F = 3/2$ states while, in ${}^{40}\text{K}$, it is formed from $|\frac{7}{2} - \frac{7}{2}\rangle$ and the lowest eigenstate $|\frac{9}{2} - \frac{9}{2}\rangle$.

tion operators, $\{\beta_{ki}, \beta_{\bar{k}i}\}$, in terms of the *particle* creation and annihilation operators, via the Bogoliubov-Valatin transformation [9]. Then, the ground state, $|\Phi\rangle$, of the Hamiltonian (1), is obtained via a variational ansatz, such that $\beta_{ki}|\Phi\rangle = 0$, for all $\{ki\}$ labels. We will refer to this state as the HFB wave function.

While the above approach is general for any arbitrary multi-level fermionic Hamiltonian [10], for the purpose of the present discussion we will confine ourselves to a two level (one-channel) model, such as discussed in [11, 12]. In this model the HFB wave function has the BCS form

$$|\Phi\rangle = \prod_{\mathbf{k}} \left(u_{\mathbf{k}} + v_{\mathbf{k}} a_{\mathbf{k}\uparrow}^\dagger a_{-\mathbf{k}\downarrow}^\dagger \right) |0\rangle, \quad (3)$$

subject to the normalization condition,

$$|u_{\mathbf{k}}|^2 + |v_{\mathbf{k}}|^2 = 1. \quad (4)$$

For zero magnetic field, B , the states $|\uparrow\rangle$ and $|\downarrow\rangle$ refer to the two fermion types $|F M_F\rangle \equiv |\frac{3}{2}, \frac{1}{2}\rangle$ and $|\frac{3}{2}, -\frac{1}{2}\rangle$ for ${}^6\text{Li}$, and $|\frac{7}{2}, -\frac{7}{2}\rangle$ and $|\frac{9}{2}, -\frac{9}{2}\rangle$ for ${}^{40}\text{K}$. For finite values of B , we have

$$\begin{aligned} "|\uparrow\rangle" &= a |11\rangle |\downarrow\rangle + b |10\rangle |\uparrow\rangle \xrightarrow{B \rightarrow 0} |\frac{3}{2}, \frac{1}{2}\rangle, \\ "|\downarrow\rangle" &= c |10\rangle |\downarrow\rangle + d |1-1\rangle |\uparrow\rangle \xrightarrow{B \rightarrow 0} |\frac{3}{2}, -\frac{1}{2}\rangle, \end{aligned} \quad (5)$$

TABLE I: Parameters entering the modified Pauli matrices.

Atom	a	b	c	d	$(b^2 - a^2)$	$(d^2 - c^2)$	bc
[B = 0]							
${}^6\text{Li}$	$\frac{1}{\sqrt{3}}$	$\sqrt{\frac{2}{3}}$	$\sqrt{\frac{2}{3}}$	$\frac{1}{\sqrt{3}}$	$\frac{1}{3}$	$-\frac{1}{3}$	$\frac{2}{3}$
${}^{40}\text{K}$	$\frac{1}{3}$	$-\frac{2\sqrt{2}}{3}$	1	0	$\frac{7}{9}$	-1	$-\frac{2\sqrt{2}}{3}$
[B \rightarrow ∞]							
${}^6\text{Li}$	0	1	0	1	1	1	0
${}^{40}\text{K}$	1	0	1	0	-1	-1	0

for ${}^6\text{Li}$, while for ${}^{40}\text{K}$ we have

$$\begin{aligned} "|\uparrow\rangle" &= a |4-3\rangle |\downarrow\rangle + b |4-4\rangle |\uparrow\rangle \xrightarrow{B \rightarrow 0} |\frac{7}{2} - \frac{7}{2}\rangle, \\ "|\downarrow\rangle" &= |4-4\rangle |\downarrow\rangle \xrightarrow{B \rightarrow 0} |\frac{9}{2} - \frac{9}{2}\rangle. \end{aligned} \quad (6)$$

The parameters (a, b, c, d) are related to the hyperfine mixing angles, such that

$$a = \sin \phi_1, \quad b = \cos \phi_1, \quad c = \sin \phi_2, \quad d = \cos \phi_2, \quad (7)$$

for ${}^6\text{Li}$, and

$$a = \cos \phi_1, \quad b = \sin \phi_1, \quad c = \cos \phi_2, \quad d = \sin \phi_2, \quad (8)$$

for ${}^{40}\text{K}$. When the magnetic field is zero, the above parameters are given by the appropriate Clebsch-Gordan coefficients, while for large fields we retrieve the unmixed phase, as illustrated in Table I.

The ground-state properties are described by the *normal* and *anomalous* densities defined as

$$\rho_{\mathbf{k}} = \langle \Phi | \mathbf{a}_{\mathbf{k}\uparrow}^\dagger \mathbf{a}_{\mathbf{k}\uparrow} | \Phi \rangle = |v_{\mathbf{k}}|^2, \quad (9)$$

$$\kappa_{\mathbf{k}} = \langle \Phi | \mathbf{a}_{-\mathbf{k}\downarrow} \mathbf{a}_{\mathbf{k}\uparrow} | \Phi \rangle = v_{\mathbf{k}}^* u_{\mathbf{k}}, \quad (10)$$

while the mean total particle-density of the system, ρ_0 , is given by

$$\rho_0 = \langle \Phi | \hat{N} | \Phi \rangle = 2 \int \frac{d^3k}{(2\pi)^3} \rho_{\mathbf{k}}. \quad (11)$$

The ground-state ansatz (3) provides a smooth interpolation between the BCS and the BEC regimes. We have recently [12] used this model to study the properties of the BEC-BCS crossover, for a short- (but finite) range and attractive interaction. In the dilute limit the model is equivalent to the zero-range (contact) interaction Hamiltonian, initially discussed by Leggett [13]. The study presented in Ref. [12] was carried out by modifying the scattering length of the interaction, while keeping the density and range of the interaction fixed. Figure 2 illustrates the momentum distributions of the normal and anomalous densities. The mean-field solution predicts the crossover occurs when the minimum in the quasi-particle energy spectrum shifts from a finite (BCS) to zero-momentum value (BEC). As such, the presence/absence of the singularity in the momentum distribution of the density of states represents a unambiguous signature of the crossover (see inset in Fig.1).

Here, we focus on the changes in the two-point correlation functions as we evolve the system from the BEC to the BCS regimes. We begin by defining the response functions

$$S_\rho(q) = \frac{1}{\rho_0} \int [d^3\xi] e^{i\mathbf{q}\cdot\xi} \langle \Phi | \rho(\mathbf{r}) \rho(\mathbf{r}') | \Phi \rangle |_{\xi=\mathbf{r}-\mathbf{r}'}, \quad (12)$$

$$S_\sigma^{\mu\nu}(q) = \frac{1}{\rho_0} \int [d^3\xi] e^{i\mathbf{q}\cdot\xi} \langle \Phi | S_\mu(\mathbf{r}) S_\nu(\mathbf{r}') | \Phi \rangle |_{\xi=\mathbf{r}-\mathbf{r}'}, \quad (13)$$

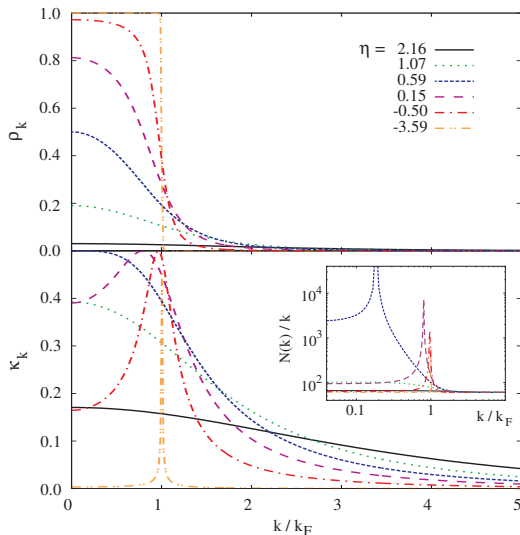


FIG. 2: (Color online) Momentum distribution of the normal and anomalous densities, as a function of the scattering length, at fixed system density, ρ_0 ($k_F \langle r \rangle \approx 0.37$). Inset shows the density of states. We use the notation $\eta = (a_0 k_F)^{-1}$.

where $\rho(\mathbf{r})$ and $S_\mu(\mathbf{r})$ denote the particle- and spin-density operators

$$\rho(\mathbf{r}) = \sum_{ij} \mathbf{a}_i^\dagger \langle i | \delta(\mathbf{r} - \mathbf{r}_1) | j \rangle \mathbf{a}_j, \quad (14)$$

$$S_\mu(\mathbf{r}) = \frac{1}{2} \sum_{ij} \mathbf{a}_i^\dagger \langle i | \sigma_\mu \delta(\mathbf{r} - \mathbf{r}_1) | j \rangle \mathbf{a}_j. \quad (15)$$

Here, σ_μ denote the Pauli matrices. Since the single-particle states are plane waves, i.e. $|i\rangle = e^{i\mathbf{k}_i \cdot \mathbf{r}} \chi_i$, where χ denotes the ($|\uparrow\rangle$, $|\downarrow\rangle$) spinors, then we can calculate the particle-density matrix element as

$$\langle i | \delta(\mathbf{r} - \mathbf{r}_1) | j \rangle = \delta_{ij} e^{i(\mathbf{k}_j - \mathbf{k}_i) \cdot \mathbf{r}}, \quad (16)$$

and the spin-density matrix element as

$$\langle i | \sigma_\mu \delta(\mathbf{r} - \mathbf{r}_1) | j \rangle = \langle \chi_i | \sigma_\mu | \chi_j \rangle e^{i(\mathbf{k}_j - \mathbf{k}_i) \cdot \mathbf{r}}. \quad (17)$$

The density response function in (12) is a scalar, while the spin density response function in (13) is a tensor. For the one-channel model the spin-response tensor is diagonal, and, provided that the Hamiltonian and the total spin operator commute, the diagonal components are equal. Then, the density and spin response functions correspond to the sum and difference of *separate* normal and anomalous density contributions, respectively. The nonlocal response functions can be written as

$$S_\rho(q) \doteq \mathcal{I}_\kappa(q) - \mathcal{I}_\rho(q), \quad (18)$$

$$S_\sigma(q) \doteq -\frac{1}{4} [\mathcal{I}_\kappa(q) + \mathcal{I}_\rho(q)]. \quad (19)$$

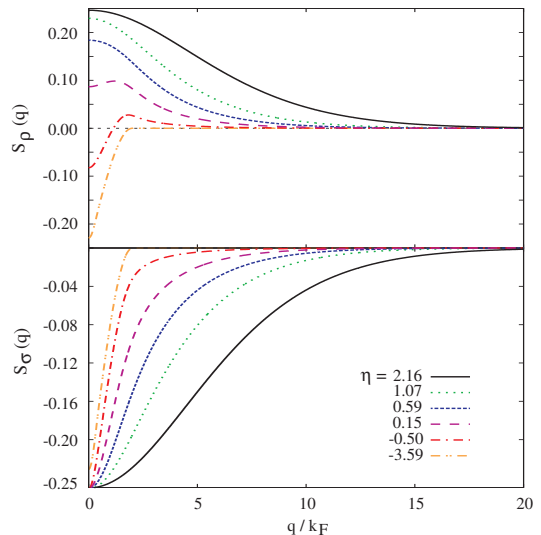


FIG. 3: (Color online) The density and spin instantaneous response function for an electron gas, as a function of the scattering length (or $\eta = (a_0 k_F)^{-1}$), at fixed density, ρ_0 .

Equations (18) and (19) represent a general result for the HFB mean-field approximation of the ground-state of the multi-level Hamiltonian (1). For the one-channel model, and disregarding for now the hyperfine nature of the atomic levels involved (similarly to the case of an electron gas), the normal and anomalous density contributions to the response functions are:

$$\mathcal{I}_\rho(q) = \frac{2}{\pi^3 \rho_0} \int_0^\infty d\xi \xi^2 j_0(\xi q) \left[\int_0^\infty dk k^2 \rho_k j_0(\xi k) \right]^2, \quad (20)$$

$$\mathcal{I}_\kappa(q) = \frac{2}{\pi^3 \rho_0} \int_0^\infty d\xi \xi^2 j_0(\xi q) \left[\int_0^\infty dk k^2 \kappa_k j_0(\xi k) \right]^2. \quad (21)$$

The response functions $S_\rho(q)$ and $S_\sigma(q)$ are shown in Fig. 3. The density response function, $S_\rho(q)$, changes sign at low momentum, as the bound state disappears, while the spin response function, $S_\sigma(q)$, changes smoothly from the BEC to the BCS regime. In the BCS limit, the condensate wave function, κ_k , appears in a very narrow region around the Fermi momentum (see Fig. 2). Since the width of this distribution tends to zero in the limit $a_0 \rightarrow -0$, so does the anomalous density contribution, $\mathcal{I}_\kappa(q)$. In turn, the density and spin response functions will be equal in this limit.

The mean-field approach shows that a measurement of the density response function is a signature of the BEC-BCS crossover. In the dilute limit, the crossover coincides with the singularity in the scattering length, which in turn corresponds to the change in sign of the density response function. Figure 4 (top) shows the dependence of $\mathcal{I}_\kappa(q)$ and $\mathcal{I}_\rho(q)$ for $q = 0$, as a function of the scattering length a_0 at fixed density ρ_0 ($k_F \langle r \rangle \approx 0.37$). The corresponding density response function $S_\rho(0)$ is depicted in Fig. 4 (bottom). The density response function changes

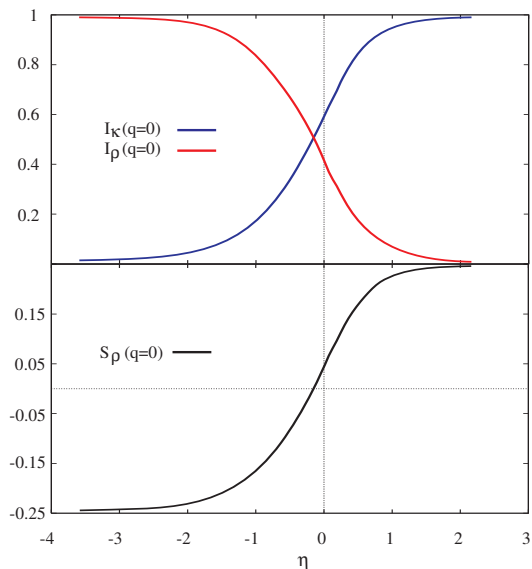


FIG. 4: (Color online) Zero-momentum transfer normal and anomalous density contributions, $\mathcal{I}_\kappa(0)$ and $\mathcal{I}_\rho(0)$, together with the density response function $S_\rho(q)$ for $q = 0$.

sign between the BCS and the BEC limits.

The one-channel model predicts that the spin response function at zero momentum transfer, $S_\sigma(q = 0)$, is in fact a sum rule, i.e.

$$S_\sigma(0) = -\frac{1}{4\pi^2\rho_0} \int_0^\infty dk k^2 (\kappa_k^2 + \rho_k^2) = -\frac{1}{4}, \quad (22)$$

or $\mathcal{I}_\rho(0) + \mathcal{I}_\kappa(0) = 1$ is independent of $\eta = (a_0k_F)^{-1}$, as shown in Fig. 4 (top). The above is obtained by using the definitions (9) and (10), together with the normalization condition, Eq. (4).

We now consider the modification of the electron gas results, due to the hyperfine nature of the interacting atomic levels. We find the spin response function is proportional to the “weighted” difference of the normal and anomalous density contributions derived earlier, $\mathcal{I}_\kappa(q)$ and $\mathcal{I}_\rho(q)$. The weighting factors depend on the atom specie in the system, and the atomic levels involved in the interaction. Since the spin response function is only sensitive to the electron spin operator, then in order to find the modification of the spin response function, we need to calculate the matrix elements $\langle\chi_i|\sigma_\mu|\chi_j\rangle$ in Eq. (17). The parameters entering the modified Pauli matrices are

$$\sigma_0 \rightarrow \begin{pmatrix} b^2 - a^2 & 0 \\ 0 & d^2 - c^2 \end{pmatrix}, \quad \sigma_\pm \rightarrow bc \sigma_\pm, \quad (23)$$

and limiting values as a function of the magnetic field, B , are listed in Table I. We note that in the large field limit, the spin response in a ${}^6\text{Li}$ fermionic atom gas has opposite sign as compared to the case of a ${}^{40}\text{K}$ fermionic atom gas. Irrespective of the actual B value, we obtain that for a fermionic atom gas, the rotational symmetry

of the spin response function is broken. This symmetry-breaking effect is a prediction of our model, and arises as a consequence of the fact that our effective interaction involves a restricted set of atomic levels.

In conclusion, in this paper, we have shown that much information about the crossover regime can be gained by experimentally studying the density and spin response functions. Within the framework of the mean-field results, we show that the normal and anomalous densities can be accessed from the momentum distribution of the response functions. The spin response function changes smoothly across the crossover, while the density response function changes sign, and thus represents a signature of the crossover. The spin response at zero-momentum transfer satisfies a sum rule, and is sensitive to the interaction. When taking into account the hyperfine structure of the interacting levels, our model predicts that the rotational invariance of the spin response, normally associated with an electron gas subject to a spin-independent interaction, is broken.

-
- [1] J. Kinast *et al.*, Phys. Rev. Lett. **92**, 150402 (2004); M. Bartenstein *et al.*, *ibid.* **92**, 203201 (2004); C. Chin *et al.*, Science **305**, 1128 (2004).
 - [2] S. Jochim *et al.*, Science **302**, 2101 (2003); M. Greiner, C. A. Regal, and D. S. Jin, Nature (London) **426**, 537 (2003); M. W. Zwierlein *et al.*, Phys. Rev. Lett. **91**, 250401 (2003); M. Bartenstein *et al.*, *ibid.* **92**, 120401 (2004); T. Bourdel *et al.*, *ibid.* **93**, 050401 (2004).
 - [3] M. R. Shafroth, S. T. Butler, and J. M. Blatt, Helv. Phys. Acta, **30**, 93 (1957); M. R. Shafroth, Phys. Rev. **111**, 72 (1958); P. Nozières and S. Schmitt-Rink, J. Low Temp. Phys. **59**, 195 (1985); Y. I. Uemura *et al.*, Phys. Rev. Lett. **66**, 2665 (1991); V. M. Loktek, R. M. Quick, and S. G. Sharapov, Phys. Repts. **349**, 1 (2001).
 - [4] C. A. Regal, M. Greiner, and D. S. Jin, Phys. Rev. Lett. **92**, 040403 (2004).
 - [5] M. W. Zwierlein *et al.*, Phys. Rev. Lett. **92**, 120403 (2004).
 - [6] L. Viverit *et al.*, Phys. Rev. A **69**, 13607 (2004).
 - [7] G. M. Bruun and G. Baym, Phys. Rev. Lett. **93**, 150403 (2004).
 - [8] E. Altman, E. Demler, and M. D. Lukin, Phys. Rev. A **70**, 13603 (2004).
 - [9] N. N. Bogoliubov, Nuovo Cimento **7**, 794 (1958); J. G. Valatin, Nuovo Cimento **7**, 843 (1958); J. G. Valatin, Phys. Rev. **122**, 1012 (1961).
 - [10] M. M. Parish, B. Mihaila, B. D. Simons, and P. B. Littlewood, e-print cond-mat/0409756.
 - [11] C. Comte and P. Nozières, J. Phys. (Paris) **43**, 1069 (1982); P. B. Littlewood and X. J. Zhu, Phys. Scr. **T68**, 56 (1996).
 - [12] M. M. Parish, B. Mihaila, E. M. Timmermans, K. B. Blagojev, and P. B. Littlewood, Phys. Rev. B (in press), e-print cond-mat/0410131.
 - [13] A.J. Leggett, in *Modern Trends in the Theory of Condensed Matter*, edited by A. Pekalski and R. Przystawa (Springer-Verlag, Berlin, 1980).